SAND2021-15423C

Demonstration of a Burst-Mode-Pumped Noncolinear Optical Parametric Oscillator (NOPO) for Broadband CARS Diagnostics in Gases

Elijah R. Jans[1], Sean P. Kearney[2], and Darrell J. Armstrong[3]
Sandia National Laboratories, Albuquerque, NM 87185

Arlee V. Smith[4]
AS-Photonics, LLC, 6916 Montgomery Blvd. NE, Suite B8, Albuquerque, NM 87109 USA

Demonstration of broadband nanosecond output from a burst-mode-pumped noncolinear optical parametric oscillator (NOPO) has been achieved at 40 kHz. The NOPO is pumped by 355-nm output at 50 mJ/pulse for 45 pulses. A bandwidth of 540 cm^{-1} was achieved from the OPO with a conversion efficiency of 10% for 5 mJ/pulse. Higher bandwidths up to 750 cm^{-1} were readily achievable at reduced performance and beam quality. The broadband NOPO output was used for a planar BOXCARS phase matching scheme for N_2 CARS measurements in a near adiabatic H_2/air flame. Single-shot CARS measurements were taken for equivalence ratios of φ=0.52-0.86 for temperatures up to 2200 K.

I. Introduction

A basic understanding of chemical kinetics, molecular energy transfer, and thermodynamics in dynamic, high-speed engineering applications—such as nonequilibrium reacting flows, hypersonic systems, and detonation of energetic materials—is a key driver for modern laser-based diagnostics [1, 2]. Laser-based approaches, such as particle-image velocimetry (PIV); Doppler velocimetry; planar laser induced fluorescence (PLIF); Thomson/Raman/Rayleigh scattering; and numerous four-wave mixing approaches have been utilized to probe gas-phase applications in combustion, plasma science, and fluid dynamics for the past several decades [3, 4]. These powerful space- and time-resolved measurement approaches have, to a large degree, utilized Nd:YAG and YAG-pumped dye laser and optical parametric oscillator (OPO) systems, which are generally limited to pulse repetition rates to ~10 Hz at the required pulse energies for diagnostics. More recent advances have pushed data rates to 1–5 kHz by using femtosecond Ti:sapphire amplifiers for techniques such as coherent anti-Stokes Raman scattering (CARS) [5-9]; PLIF [10, 11]; and molecular tagging velocimetry [12, 13]. The high-speed applications alluded to above feature dynamics in the 100s of kHz to MHz range, often with facility run times that are only a few hundred microseconds to milliseconds—both of which require much higher data rates than traditional diagnostic platforms have delivered. Burst-mode Nd:YAG lasers [14, 15] overcome the ~10-Hz repetition-rate barrier associated with repetitively pulsed systems, by overdriving the gain medium at very low duty cycle, allowing sufficient time between bursts for thermal management. These exciting new laser platforms were first demonstrated for high-speed flow visualization and PIV [16], where only the

[1] Post-doctoral Appointee, Engineering Sciences Center, erjans@sandia.gov, AIAA Member.
[2] Distinguished Member of the Technical Staff, Engineering Sciences Center, spkearn@sandia.gov, AIAA Associate Fellow.
[3] Principal Member of the Technical Staff, Pulsed Power Sciences Center.
[4] Owner and CEO.

532-nm Nd:YAG second harmonic was required, but these high-speed Nd:YAG sources were quickly coupled to frequency tunable OPOs for chemically specific PLIF diagnostics of NO [17], OH [18] , and CH_2O [19].

Coherent anti-Stokes Raman scattering (CARS) has a demonstrated history of high-precision thermometry [20-23] across a wide range of temperatures. The technique has very recently been adapted to a pulse-burst laser platform to demonstrate 100-kHz rate thermometry by Roy *et al.* [24]. The chief technical barrier for high-speed CARS diagnostics is development of a broadband (100 cm^{-1} FWHM or more) source that is tunable in the visible spectrum. Roy *et al.* [24] have utilized a burst-mode laser that delivers ~100-ps pulses to achieve sufficient pulse intensities for efficient optical parametric generation (OPG) in BBO. Their picosecond OPG source was combined with subsequent optical parametric amplification (OPA) to generate 2.3-mJ laser pulses with ~200 cm^{-1} FWHM bandwidth centered near 680 nm for CARS of the H_2 molecule. This picosecond OPG/OPA scheme has very recently been applied for N_2 CARS thermometry at 100 kHz [25]. While an enabling technology for 100-kHz CARS thermometry, the poor coherence of broadband picosecond pulses combines with the short lifetime of the picosecond CARS signal pulse to yield CARS spectra with poor single-laser-shot noise characteristics. Smyser *et al.* [26] have very recently demonstrated a new combined femtosecond/picosecond burst-mode laser system, for "hybrid" pure-rotational CARS measurements in room-temperature N_2. This system has great potential because the near-transform-limited performance of femtosecond laser pulses delivers superior low-noise pump/Stokes preparation relative to a picosecond broadband source, but the 270-fs pulses delivered by this burst-mode system do not yet provide sufficient bandwidth (~50 cm^{-1}) for high-temperature applications.

The objective of the work reported here is the demonstration of burst-mode CARS thermometry at data rates of 40 kHz using nanosecond laser pulses. Nanosecond-duration laser pulses have a proven track record for CARS thermometry with precision approaching 3% [27]. Broadband Stokes sources for nanosecond CARS at 10 Hz are typically generated using dye lasers and suffer from similarly poor coherence to their picosecond counterparts discussed above; however, nanosecond-duration laser pulses sample the induced Raman coherence a much longer time, resulting in an averaging of the CARS spectrum over ~100 Raman lifetimes or more in high-temperature applications. We have constructed a broadband, burst-mode-pumped OPO, which is widely tunable throughout the visible spectrum and can deliver up to 5 mJ/pulse and several hundred cm^{-1} FWHM bandwidths when pumped by 10-ns pulses at 355-nm from a burst-mode Nd:YAG laser. The burst-mode-pumped OPO uses a noncollinear geometry to produce an output beam with large spectral bandwidths [28]. The bandwidth for parametric amplification is to first order the inverse of the temporal walk off between the signal and idler waves due to the differing group velocities. If the group velocities can be made equal the bandwidth is limited by the second order dispersive effect of group velocity dispersion. The signal and idler wavelengths are 590 nm and 891 nm in one case and 607 nm and 855 nm in the second case. The idler waves have higher group velocities than their partner signal waves. The effective group velocity of the idler light can be slowed by tilting the beams as shown in the k-vector diagram of Figure 1. The signal wave is resonated in the OPO cavity so its k-vector must be parallel the cavity axis. By tilting the 355 nm pump beam relative to the cavity axis the k-vector of the idler beam must also tilt to achieve phase matching. With the right choice of pump angle the group velocity of the idler beam as measured parallel to the cavity axis will match the signal group velocity, maximizing the bandwidth of both generated beams. For o-polarized signal and idler beams and e-polarized pump beam in a BBO crystal group velocity matching is achieved with a pump beam k-vector tilt of 4.1 degrees relative to the cavity axis for both the signal wavelengths. The Poynting vector of the e-polarized 355 nm beam tilts by 4.35 degrees relative to its k-vector due to birefringent walk off. The correct choice of the sign of the pump beam tilt relative to the cavity axis leads to a power flow (Poynting vector) of the pump light that is nearly parallel to that of the signal beam. Ideally, the idler beam is angle dispersed, as shown in the k-vector diagram, while the signal beam is not. In practice, the large diameter and single pass of the pump beam allows slight angular dispersion of the signal beam as well.

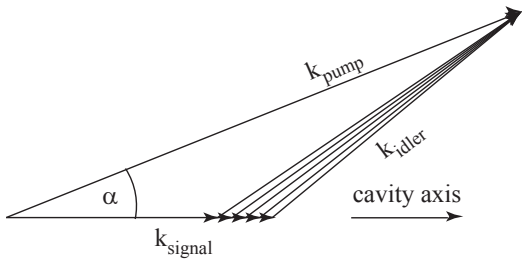

Fig. 1: Phase matching diagram for non-collinearly pumped OPO. The signal beam is parallel to the OPO cavity axis; the pump is tilted by angle α from the cavity axis; the idler beam is angle dispersed to close the k-vector triangle. With the right value of α, the group velocities of the signal and idler parallel to the cavity axis are equal and the bandwidth is maximal.

II. Experimental Set-up

The experimental set-up for the CARS system, including the burst-mode-pumped NOPO, is shown in Figure 2. A Spectral Energies "Quasimodo" burst-mode laser provides both 532- and 355-nm, 10-ns pulses at 40 kHz. The laser was operated with a pulse width of 10 ns for a total burst duration of 1.5 ms. The NOPO is pumped at 355 nm and 50 mJ/pulse, with 45 total pulses in the burst. This 355-nm pump beam is down-collimated by a 2:1 telescope and the resulting OPO pump is 3-mm in diameter. The OPO cavity is ~90-mm long, and is formed by two flat mirrors mounted on a rotary stage, with an intra-cavity pump mirror and Type-I β-barium-borate (BBO) crystal each mounted on platforms independent from the cavity rotary stage. In this manner, the OPO cavity axis can be independently rotated with respect to the input 355-nm pump beam and the BBO crystal. The uncoated BBO crystal is 10 mm × 10 mm across its face and 12 mm in length and is cut with its optical axis at 32.8° to the crystal face. The signal-resonant cavity is composed of a high reflector for wavelengths λ = 598–610 nm and an output coupler with R=65% for 598-610 nm and high transmission at λ = 355 nm. The OPO is initially aligned with the pump axis perpendicular to the cavity mirrors in a typical colinear phase-matched OPO configuration. The cavity is then tilted gradually while observing the output spectrum of the OPO signal beam and compensating the angle of the BBO crystal to keep the center frequency of the signal wave in the desired position.

The CARS system is configured in a planar BOXCARS phase matching scheme [30] with the 532-nm beam from the burst-mode laser split by a 50/50 beam splitter to provide two CARS pump beams and the broadband output from the NOPO used as the Stokes beam. Thermometry was demonstrated in the product gases of near-adiabatic H_2/air flat flames, stabilized on a Hencken-type burner with a 5-cm × 5-cm substrate, with the CARS measurement volume positioned 10 mm above the burner surface. The ~473-nm CARS signal is separated from the intense pump-beam radiation using several 473-nm high reflectors and two bandpass filters centered at 470 nm with a 20 nm FWHM. A 0.5 meter spectrometer (Princeton Instruments SpectraPro HRS-500) with an electron-multiplying (EM) CCD camera (Princeton Instruments Pro-EM-HS 1024) was used to acquire the CARS signal. The EM-CCD enables fast, 40-kHz acquisition of spectra by vertically shifting charge on each successive laser shot and using the entire 1024×1024 pixel chip and an adjacent 1024×1024 pixel masked area to store all information accumulated during the 45-pulse burst prior to sensor readout. This type of camera has previously been demonstrated for burst-mode CARS at 100-kHz rates [24, 25] and spontaneous-Raman scattering at 10 kHz [31]. The measurement length, determined by propagating a glass coverslip through the focal point, incorporating 90% of the generated signal occurred within 17 mm.

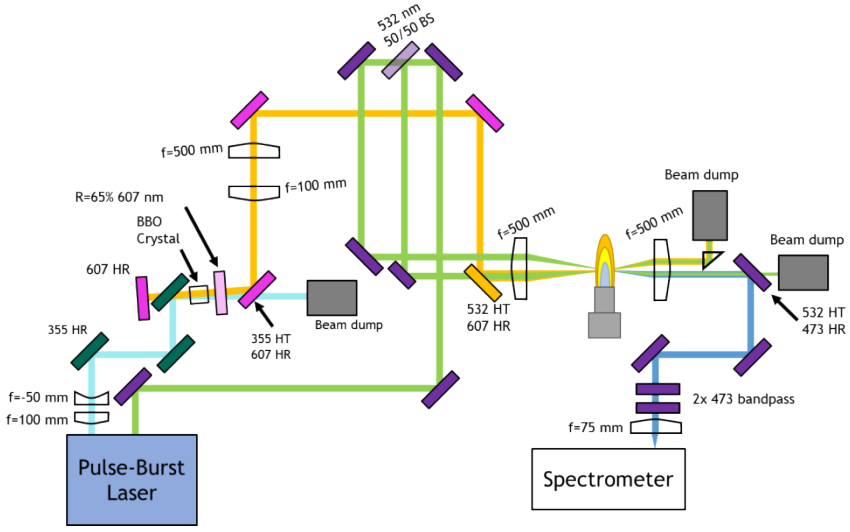

Fig. 2 Schematic of the NOPO and CARS experiment with a Hencken burner.

III. Results and Discussion

Representative OPO spectra at center wavelengths for N_2 (λ_o = 607 nm) and O_2 (λ_o = 590 nm) for CARS spectroscopy with a 532-nm pump beam are shown in Figure 3. The spectra were measured with an Ocean Optics spectrometer (QE65000) with a spectral resolution of 20 cm^{-1} and represent single-laser-shot measurements with the NOPO pumped at 10 Hz by an injection-seeded Nd:YAG laser. Frequency narrow spectra obtained in collinear phase-matched operation are shown as black curves, while broadband spectra were obtained in the NOPO configuration are

shown in blue and red. Least-squares fits of single-shot data, shown by the dashed curves on the plot, indicated FWHM bandwidths of 360 cm^{-1} and 428 cm^{-1}, respectively, with the bandwidth generally increasing as the BBO crystal is tuned to the red and closer to the OPO degeneracy point, where the group velocity of the signal and idler are, by definition, identical. Output bandwidths up to 700 cm^{-1} could readily be achieved, with reductions in both pulse energy and beam quality.

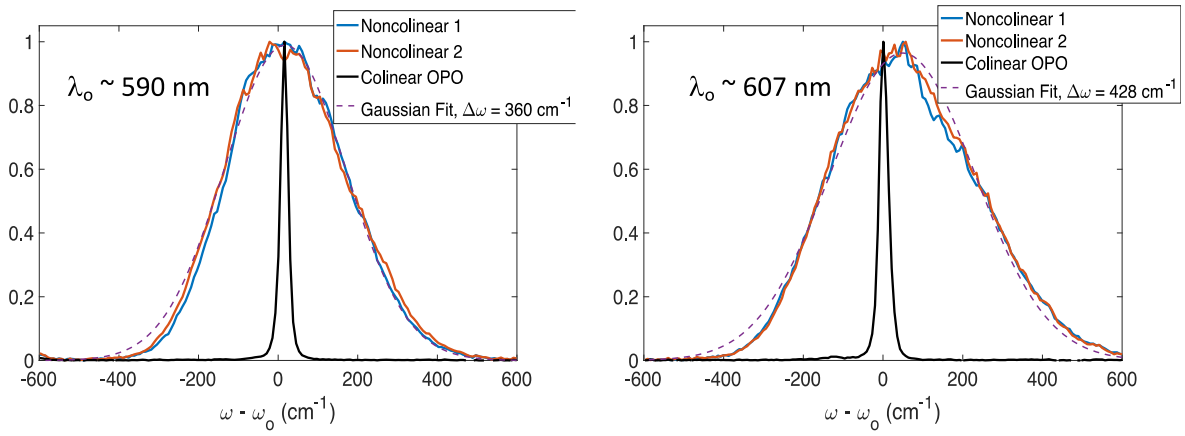

Fig. 3 Broadband (blue and red) and frequency-narrow (black) output spectra obtained in NOPO and colinear arrangements, respectively. The spectra illustrate the tunability of the NOPO device for both O_2 (590 nm) and N_2 (607 nm) CARS.

The NOPO configuration was additionally pumped with the burst-mode system at 40 kHz. A representative burst-mode-pumped spectrum is shown Figure 4, where the broadband output of the OPO has been averaged over the entire 45-pulse burst. A Gaussian profile was fit to the OPO output for a FWHM of 540 cm^{-1} (20 nm). Burst profiles for both the 355-nm pump (black) and 607-nm NOPO output (red) are shown in Figure 5, where pulse uniformity of the NOPO pulse through the short 45-pulse burst is generally observed to be excellent. For a 45-pulse burst of 355-nm pump pulses at 50 mJ/pulse, the output energy from the OPO at 607 nm beam was 5 mJ/pulse, for a conversion efficiency of 10%. From Figure 5, it is shown that the pulse energy from the NOPO is nearly uniform throughout the burst.

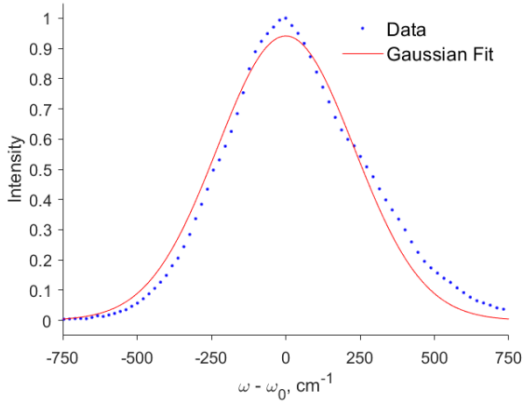

Fig. 4 Output from the BBOPO at 607 nm being pumped at pulse repetition rate of 40 kHz with a cavity angle of about 5°. The output is fit with a Gaussian lineshape with inferred FWHM of 540 cm^{-1}.

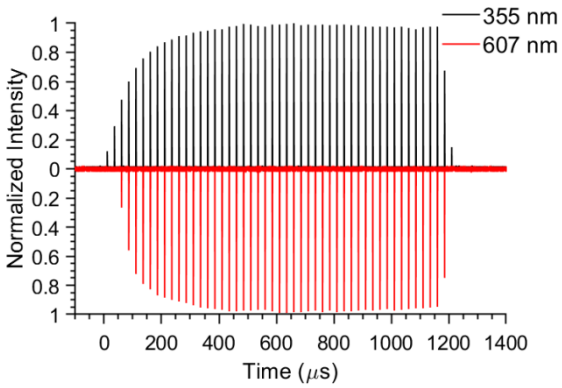

Fig. 5 Relative intensities of the 355 nm and 607 nm beams at 40- kHz pulse repetition rate.

The NOPO center wavelength was tuned to $\lambda = 607$ nm for N_2 Raman detection with a BOXCARS phase matching scheme, as shown in Figure 2. The nonresonant background (NRB) spectrum taken in argon, averaged over 15 bursts at a pulse rate of 40 kHz for 45 pulses is shown in Figure 6. It was observed that the 370-cm^{-1}-wide NRB spectrum contained less bandwidth than the 540-cm^{-1} NOPO output, shown in Figure 4, which is likely due to the angular dispersion of the signal beam resulting from noncollinear phase matching. From burst to burst, the NRB had a central wavelength variation of 30 cm^{-1} and had a bandwidth variation of 18 cm^{-1} over the 15 bursts. Typical single-shot CARS measurements are shown in Figure 7 and were taken in a near adiabatic H_2-air flame from a Hencken burner with a range of equivalence ratios from φ=0.52-0.86. Good single-shot signal-to-noise was observed over a wide range of flame temperatures, even with a relatively modest 5-mJ/pulse Stokes source energy. The noise in these single-shot CARS spectra is largely dominated by NOPO photon statistics. The burst-mode laser used in this work is expected to exhibit near-transform-limited performance, so that pump laser statistics are not a significant contributor to the observed CARS noise. In principle, the Stokes source noise can be reduced by increasing the NOPO oscillator cavity length from ~9-cm to 30-cm or more, which is typical of nanosecond broadband dye laser systems used for gas-phase CARS. The longer cavity reduces longitudinal mode spacing, thereby increasing the number of modes interacting with a given Raman resonance [32]. Use of a longer NOPO cavity will result in higher oscillation thresholds for pump energy and reduced NOPO power, which may be overcome by adding parametric amplifiers to the Stokes source design.

Gas temperatures were inferred from the CARS measurements using a least-squares fit to a library of spectra generated by CARSFT [33]. The inferred temperature for five different equivalence ratios from $\phi = 0.52$ to 0.86 is shown in Figure 8. The orange circles represent the mean temperature from 400 single-laser-shot realizations, while the error bars indicate the corresponding standard deviation in the temperature measurements. The observed single-shot measurement precision (one standard deviation) was 4.9% of the mean temperature at $T = 1696$ K to 5.7% of mean at $T = 2126$ K. Mean CARS-measured temperatures were within 1.85% of equilibrium. Uncertainties in gas flow rates were accounted for by shifting the equivalence ratio axis in Figure 8 by 0.105 for a best match agreement of the measured temperature curve to calculated adiabatic flame temperatures. The observed measurement precision is degraded by ~1.6–2× relative to the 3% levels attained with 10-Hz nanosecond vibrational CARS under ideal laboratory conditions [34, 35] with single-mode pump lasers, but is comparable to some vibrational CARS measurements using multimode pump lasers [34] as well as some early reports of pure-rotational nanosecond CARS thermometry in flames [27]. The observed precision of flame temperatures using the burst-mode-pumped ns-NOPO are close to the values reported in [25] obtained with a burst-mode pumped ps-OPG with shot-to-shot NRB corrections. Comparing the two demonstrations of pulse-burst CARS measurements, the nanosecond NOPO system has several advantages: less complexity, exhibits lower inherent noise, and has the potential to approach the precision seen in 10-Hz CARS systems.

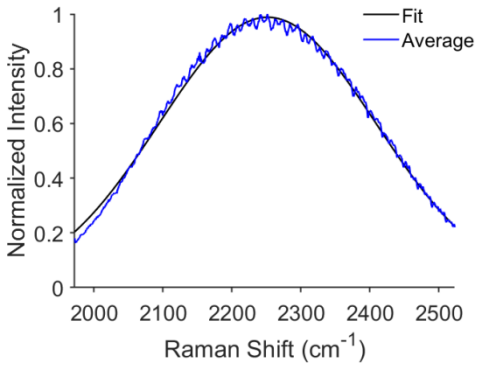

Fig. 6 Nonresonant background taken in argon for an average of 15 bursts with a Gaussian fit of FWHM =370 cm^{-1}.

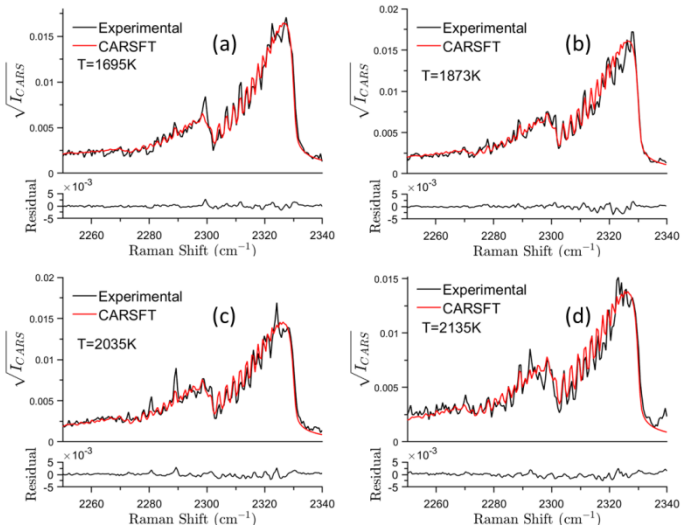

Fig. 7: Single shot CARS signal from a 40 kHz pulse repetition rate burst in a Hencken burner flame fit with CARSFT for equivalence ratios of (a) φ=0.52, (b) φ=0.61, (c) φ=0.69, and (d) φ=0.77.

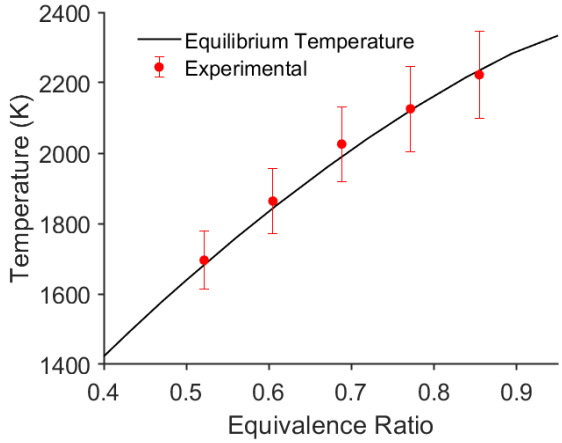

Fig. 8: CARS temperature inferred from single-shot data for 400 shots using five different equivalence ratios from a near-adiabatic H_2/air Hencken Burner flame.

IV. Conclusion

We have demonstrated a broadband burst-mode-pumped NOPO for single-shot 40-kHz CARS thermometry. Stokes bandwidths as high as 370 cm^{-1} were coupled to the CARS process. Even higher bandwidths were produced by the NOPO source but were not fully coupled to the CARS spectrum, presumably as a result of angular dispersion (spatial chirp) in the OPO signal beam. Single-laser-shot thermometry from the N_2 *Q*-branch spectrum at flame temperatures from 1700 to 2200 K have been observed with a precision of 4.9– 5.7%. Noise in these single-shot spectra is dominated by NOPO photon statistics, which can be improved by increasing the oscillator cavity length and adding additional noncolinear optical parametric amplifier (OPA) stages.

V. Acknowledgements

This paper describes objective technical results and analysis. Any subjective views or opinions that might be expressed in the paper do not necessarily represent the views of the U.S. Department of Energy or the United States Government. Sandia National Laboratories is a multi-mission laboratory managed and operated by National Technology and Engineering Solutions of Sandia, LLC., a wholly owned subsidiary of Honeywell International, Inc., for the U.S. Department of Energy's National Nuclear Security Administration under contract DE-NA0003525.

References

1. Mustafa, M. A., Parziale, N. J., Smith, M. S., and Marineau, E. C. "Nonintrusive Freestream Velocity Measurement in a Large-Scale Hypersonic Wind Tunnel," *AIAA Journal* Vol. 55, No. 10, 2917.
2. Richardson, D. R., Kearney, S. P., and Guildenbecher, D. R. "Post-detonation fireball thermometry via femtosecond-picosecond coherent anti-Stokes Raman Scattering (CARS)," *Proceedings of the Combustion Institute* Vol. 38, 2021, pp. 1657-1664.
3. Eckbreth, A. C. *Laser Diagnostics for Combustion Temperature and Species*: Gordon and Breach, 1996.
4. Kohse-Höinghaus, K., and Jeffries, J. B. *Applied Combustion Diagnostics*: Taylor and Francis, 2002.
5. Miller, J. D., Slipchenko, M. N., Meyer, T. R., Stauffer, H. U., and Gord, J. R. "Hybrid femtosecond/picosecond coherent anti-Stokes Raman scattering for high-speed gas-phase thermometry," *Optics Letters* Vol. 35, No. 14, 2010, pp. 2430-2432.
6. Dennis, C. N., Slabaugh, C. D., Boxx, I. G., Meier, W., and Lucht, R. P. "5 kHz thermometry in a swirl-stabilized gas turbine model combustor using chirped probe pulse femtosecond CARS. Part 1: Temporally resolved swirl-flame thermometry," *Combustion and Flame* Vol. 173, 2016, pp. 441-453.
7. Bohlin, A., Jainski, C., Patterson, B. D., Dreizler, A., and Kliewer, C. J. "Multiparameter spatio-thermochemical probing of flame–wall interactions advanced with coherent Raman imaging," *Proceedings of the Combustion Institute* Vol. 36, 2017, pp. 4557-4564.
8. Dedic, C. E., Meyer, T. R., and Michael, J. B. "Single-shot ultrafast coherent anti-Stokes Raman scattering of vibrational/rotational nonequilibrium," *Optica* Vol. 4, No. 5, 2017, pp. 563-570.
9. Kearney, S. P. "Hybrid fs/ps rotational CARS temperature and oxygen measurements in the product gases of canonical flat flames," *Combustion and Flame* Vol. 162, No. 5, 2015, pp. 1748-1758.
10. Richardson, D. R., Jiang, N. B., Stauffer, H. U., Kearney, S. P., Roy, S., and Gord, J. R. "Mixture-fraction imaging at 1 kHz using femtosecond laser-induced fluorescence of krypton," *Optics Letters* Vol. 42, No. 17, 2017, pp. 3498–3501.
11. Richardson, D. R., Roy, S., and Gord, J. R. "Femtosecond, two-photon, planar laser-induced fluorescence of carbon monoxide in flames," *Optics Letters* Vol. 42, No. 4, 2017, pp. 875–878.
12. Michael, J. B., Edwards, M. R., Dogariu, A., and Miles, R. B. "Femtosecond Laser Excitation Tagging for Quantitative Velocity Image in Air," *Applied Optics* Vol. 50, 2011, p. 5158.
13. Miles, R. B., Michael, J. B., Limbach, C. M., McGuire, S. D., Chng, T. L., Edwards, M. R., DeLuca, N. J., Schneider, M. N., and Dogariu, A. "New diagnostic methods for laser plasma- and microwave-enhanced combustion," *Philosophical Transactions of the Royal Society of London A* Vol. 373, 2015, p. 20140338.
14. Slipchenko, M. N., Meyer, T. R., and Roy, S. "Advances in burst-mode laser diagnostics for reacting and nonreacting flows," *Proceedings of the Combustion Institute* Vol. 38, No. 1533-1560, 2021.
15. Thurow, B., Jiang, N., and Lempert, W. "Review of ultra-high repetition rate laser diagnostics for fluid dynamic measurements," *Measurement Science and Technology* Vol. 24, 2013, p. 012002.
16. Wernet, M., and Opalski, A. "Development and application of a MHz-frame rate PIV system, AIAA2004-2184," *24th AIAA Aerodynamic Measurement Technology and Ground Testing Conference*. Portland, OR, 2004.

17. Jiang, N., Webster, M., Lempert, W. R., Miller, J. D., Meyer, T. R., Ivey, C. B., and Danehy, P. M. "MHz-rate nitric oxide planar laser-induced fluorescence imaging in a Mach 10 hypersonic wind tunnel," *Applied Optics* Vol. 50, No. 4, 2011, pp. A20-A28.
18. Miller, J. D., Slipchenko, M., Meyer, T. R., Jiang, N., Lempert, W. R., and Gord, J. R. "Ultrahigh-frame-rate OH fluorescence imaging in turbulent flames using a burst-mode optical parametric oscillator," *Optics Letters* Vol. 34, No. 9, 2009, pp. 1309-1311.
19. Gabet, K. N., Patton, R. A., Jiang, N., Lempert, W. R., and Sutton, J. A. "High-speed CH2O PLIF imaging in turbulent flames using a pulse-burst laser system," *Applied Physics B* Vol. 106, 2012, pp. 569-575.
20. Kuehner, J. P., Woodmansee, M. A., Lucht, R. P., and Dutton, J. C. "High-resolution broadband N_2 coherent anti-Stokes Raman spectroscopy: comparison of measurements for conventional and modeless broadband dye lasers," *Applied Optics* Vol. 42, 2003, pp. 6757-6767.
21. Bohlin, A., Nordström, E., Carlsson, H., Bai, X. S., and Bengtsson, P. E. "Pure rotational CARS measurements of temperature and relative O_2-concentration in a low swirl turbulent premixed flame," *Proceedings of the Combustion Institute* Vol. 34, No. 2, 2012, pp. 3629-3636.
22. Beyrau, F., Seeger, T., Malarski, A., and Leipertz, A. "Determination of Temperatures and Fuel/Air Ratios in an Ethene-Air Flame by Dual-Pump CARS," *Journal of Raman Spectroscopy* Vol. 34, 2003, pp. 946-951.
23. Kearney, S. P., and Grasser, T. W. "Laser-diagnostic mapping of temperature and soot statistics in a 2-m diameter turbulent pool fire," *Combustion and Flame* Vol. 186, 2017, pp. 32-44.
24. Roy, S., Hsu, P. S., Jiang, N., Slipchenko, M. N., and Gord, J. R. "100-kHz-rate gas-phase thermometry using 100-ps pulses from a burst-mode laser," *Optics Letters* Vol. 40, No. 21, 2015, pp. 5125–5128.
25. Lauriola, D. K., Hsu, P. S., Jiang, N., Slipchenko, M. N., Meyer, T. R., and Roy, S. "Burst-mode 100 kHz N 2 ps-CARS flame thermometry with concurrent nonresonant background referencing," *Optics Letters* Vol. 46, No. 21, 2021, pp. 5489-5492.
26. Smyser, M. E., Braun, E. L., Athmanathan, V., Slipchenko, M. N., Roy, S., and Meyer, T. R. "Dual-output fs/ps burst-mode laser for megahertz-rate rotational coherent anti-Stokes Raman scattering," *Optics lLetters* Vol. 45, No. 21, 2020, pp. 5933-5936.
27. Aldén, M., Bengtsson, P.-E., Edner, H., Kröll, S., and Nilsson, D. "Rotational CARS: a comparison of different techniques with emphasis on accuracy in temperature determination," *Applied optics* Vol. 28, No. 15, 1989, pp. 3206-3219.
28. Smith, A. V. *Crystal nonlinear optics: with SNLO examples*: AS-Photonics, 2018.
29. Kobayashi, T. "Femtosecond noncollinear parametric amplification and carrier-envelope phase control," *Femtosecond Optical Frequency Comb: Principle, Operation, and Applications*. Springer, 2005, pp. 133-175.
30. Eckbreth, A. C. "BOXCARS: Crossed-beam phase-matched CARS generation in gases," *Applied Physics Letters* Vol. 32, No. 7, 1978, pp. 421-423.
31. Winters, C., Haller, T., Kearney, S., Varghese, P., Lynch, K., Daniel, K., and Wagner, J. "Pulse-burst spontaneous Raman thermometry of unsteady wave phenomena in a shock tube," *Optics Letters* Vol. 46, No. 9, 2021, pp. 2160-2163.
32. Kröll, S., Aldén, M., Berglind, T., and Hall, R. J. "Noise characteristics of single shot broadband Raman-resonant CARS with single-and multimode lasers," *Applied optics* Vol. 26, No. 6, 1987, pp. 1068-1073.
33. Palmer, R. "The CARSFT computer code calculating coherent anti-Stokes Raman spectra: User and programmer information." Sandia National Lab.(SNL-CA), Livermore, CA (United States), 1989.
34. Snelling, D., Smallwood, G., Sawchuk, R., and Parameswaran, T. "Precision of multiplex CARS temperatures using both single-mode and multimode pump lasers," *Applied optics* Vol. 26, No. 1, 1987, pp. 99-110.
35. Seeger, T., and Leipertz, A. "Experimental comparison of single-shot broadband vibrational and dual-broadband pure rotational coherent anti-Stokes Raman scattering in hot air," *Applied optics* Vol. 35, No. 15, 1996, pp. 2665-2671.